J|A|C|S
ARTICLES
Published on Web 05/17/2006

Reversible Thermal and Photochemical Switching of Liquid Crystalline Phases and Luminescence in Diphenylbutadiene-Based Mesogenic Dimers

Shibu Abraham,[†] V. Ajay Mallia,[‡] K. Vijayaraghavan Ratheesh,[†] Nobuyuki Tamaoki,*[,‡] and Suresh Das*[,†]

Contribution from the Photosciences and Photonics, Chemical Sciences and Technology Division, Regional Research Laboratory (CSIR), Trivandrum, Kerala 695019, India, and Molecular Smart System Group, Nanotechnology Research Institute, National Institute of Advanced Industrial Science and Technology (AIST), 1-1-1, Higashi, Tsukuba, Ibaraki 305-8565, Japan

Received March 7, 2006; E-mail: sdaas@rediffmail.com; n.tamaoki@aist.go.jp

Abstract: The synthesis and study of the photo- and thermoresponsive behavior of a series of novel asymmetric mesogenic dimers, consisting of a cholesterol moiety linked to a diphenylbutadiene chromophore via flexible alkyl chains are reported. These mesogenic dimers possess the combined glass forming properties of the cholesterol moiety and the photochromic and luminescent properties of the butadiene moiety. Photoinduced cis/trans isomerization of the butadiene chromophore in these materials could be utilized to bring about an isothermal phase transition from the smectic to the cholesteric state. By photochemically controlling the cis/trans isomer ratio, the pitch of the cholesteric could be continuously varied making it possible to tune the color of the film over the entire visible region, and the color images thus generated could be stabilized by converting them to N* glasses. These materials were also polymorphic, exhibiting two crystalline forms possessing distinctly different fluorescence properties. The ability to thermally switch these materials from one crystalline form to the other in a reversible manner also makes them useful for recording fluorescent images.

Introduction

Low molecular mass materials containing stimuli responsive molecules that exist in two stable and reversible chemical or physical forms have attracted much attention[1] because of their potential applications in optical memories,[2] display devices,[3] and holographic data storage.[4] With the recent advances in multimedia and development of digital versatile disk random access memory (DVD-RAM), phase change materials have come into the mainstream in optical disk technology. The fast and rewritable amorphous to crystal phase transitions of inorganic mixtures by exposure to laser beams are currently being exploited in the fabrication of commercially available DVDs.[5] Liquid crystals (LCs) form an important class of phase change materials wherein the supramolecular organization is controlled by a variety of weak noncovalent forces.[6] LC phases are highly susceptible to minor changes in their microenvironment, since the cooperative behavior of LC molecules and their long-range order help to amplify relatively weak processes occurring at the molecular level into macroscopic phenomena.[7,8] Thus, light induced phase transitions can be brought about in

[†] Photosciences and Photonics.
[‡] Molecular Smart System Group.

(1) (a) *Molecular Switches*. Feringa, B. L., Ed.; Wiley-VCH: Weinheim, 2001. (b) Yagai, S.; Karatsu, T.; Kitamura, A. *Chem.—Eur. J.* **2005**, *11*, 4054−4063. (c) Irie, M.; Fukaminato, T.; Sasaki, T.; Tamai, N.; Kawai, T. *Nature* **2002**, *420*, 759−760. (d) Kato, T. *Science* **2002**, *295*, 2414−2418. (e) Vollmer, M. A.; Clark, T. D.; Steinem, C.; Ghadiri, M. R. *Angew. Chem., Int. Ed.* **1999**, *38*, 1598−1601. (f) Li, J.; Schuster, G. B.; Cheon, K.-S.; Green, M. M.; Selinger, J. V. *J. Am. Chem. Soc.* **2000**, *122*, 2603−2612.

(2) (a) Uchida, K.; Saito, M.; Murakami, A.; Kobayashi, T.; Nakamura, S.; Irie, M. *Chem.—Eur. J.* **2005**, *11*, 534−542. (b) Chen, S. H.; Chen, H. M. P.; Geng, Y.; Jacobs, S. D.; Marshall, K. L.; Blanton, T. N. *Adv. Mater.* **2003**, *15*, 1061−1065. (c) Olson, C. E.; Previte, M. J. R.; Fourkas, J. T. *Nat. Mater.* **2002**, *1*, 225−228.

(3) (a) Aldred, M. P.; Contoret, A. E. A.; Farrar, S. R.; Kelley, S. M.; Mathieson, D.; O'Neill, M.; Tsoi, W. C.; Vlachos, P. *Adv. Mater.* **2005**, *17*, 1368−1372. (b) Pauluth, D.; Tarumi, K. *J. Mater. Chem.* **2004**, *14*, 1219−1227.

(4) (a) Yu, H.; Okano, K.; Shishido, A.; Ikeda, T.; Kamata, K.; Komura, M.; Iyoda, T. *Adv. Mater.* **2005**, *17*, 2184−2188. (b) Yamamoto, T.; Hasegawa, M.; Kanazawa, A.; Shiono, T.; Ikeda, T. *J. Mater. Chem.* **2000**, *10*, 337−342. (c) Hsiao, V. K. S.; Kirkey, W. D.; Chen, F.; Cartwright, A. N.; Prasad, P. N.; Bunning, T. J. *Adv. Mater.* **2005**, *17*, 2211−2214. (d) Jiang, G.; Michinobu, T.; Yuan, W.; Feng, M.; Wen, Y.; Du, S.; Gao, H.; Jiang, L.; Song, Y.; Diederich, F.; Zhu, D. *Adv. Mater.* **2005**, *17*, 2170−2173.

(5) (a) Kolobov, A. V.; Fons, P.; Frenkel, A. I.; Ankudinov, A. L.; Tominaga, J.; Uruga, T. *Nat. Mater.* **2005**, *3*, 703−708. (b) Naito, K. *Appl. Phys. Lett.* **1995**, *67*, 211−213. (c) Myles, A. J.; Branda, N. R. *Adv. Funct. Mater.* **2002**, *12*, 167−173.

(6) (a) Imrie, C. T.; Henderson, P. A.; Seddon, J. M. *J. Mater. Chem.* **2004**, *14*, 2486−2488. (b) Chen, B.; Zeng, X.; Baumeister, U.; Ungar, G.; Tschierske, C. *Science* **2005**, *307*, 96−99. (c) Tschierske, C. *J. Mater. Chem.* **1998**, *8*, 1485−1508. (d) Pisula, W.; Kastler, M.; Wasserfallen, D.; Robertson, J. W. F.; Nolde, F.; Kohl, C.; Müllen, K. *Angew. Chem., Int. Ed.* **2006**, *45*, 819−823. (e) Brunsveld, L.; Folmer, B. J. B.; Meijer, E. W.; Sijbesma, R. P. *Chem. Rev.* **2001**, *101*, 4071−4097. (f) Tracz, A.; Jeszka, J. K.; Watson, M. D.; Pisula, W.; Müllen, K.; Pakula, T. *J. Am. Chem. Soc.* **2003**, *125*, 1682−1683.

(7) (a) Ichimura, K. *Chem. Rev.* **2000**, *100*, 1847−1873. (b) Camacho-Lopez, M.; Finkelmann, H.; Palffy-Muhoray, P.; Shelley, M. *Nat. Mater.* **2004**, *3*, 307−310. (c) Celebre, G.; Luca, G. D.; Maiorino, M.; Iemma, F.; Ferrarini, A.; Pieraccini, S.; Spada, G. P. *J. Am. Chem. Soc.* **2005**, *127*, 11736−11744. (d) Hamley, I. W.; Castelletto, V.; Lu, Z. B.; Imrie, C. T.; Itoh, T.; Al-Hussein, M. *Macromolecules* **2004**, *37*, 4798−4807.

(8) Ikeda, T.; Nakano, M.; Yu, Y.; Tsutsumi, O.; Kanazawa, A. *Adv. Mater.* **2003**, *15*, 201−205.

 10.1021/ja061575k CCC: $33.50

LCs doped with small amounts of photoresponsive molecules,[9,10] and such systems find applications in the field of molecular electronics for development of high-speed rewritable recording devices,[11] optical data storage,[12] patterned nanostructures,[13] fluorescence imaging,[14] and band gap materials.[15] Chiral nematic (N*) LCs are especially attractive from this point of view, since in these systems the molecules self-organize into helically ordered structures which lead to selective reflection of light, depending upon the pitch of the helix. The helical pitch of N* LCs is dependent upon various factors such as temperature, electrical, or magnetic field and on the nature and concentration of impurities, which makes it possible to tune their color by a variety of external stimuli.[16]

Mesogenic dimers or twin mesogens, which consist of molecules containing two mesogenic units, are currently of great interest since they exhibit complex and novel phase behavior not usually observed in conventional LC architectures.[17] We have recently reported on dicholesteryl liquid crystals capable of forming stable glassy LCs in which the helical ordering of the N* phase is retained.[18] Glass forming LCs and in particular N* glasses have been attracting increasing attention in view of their potential application as optical filters, polarizers, and lasing materials.[19] We have shown that the dicholesteryl esters doped with photoresponsive chromophores such as azobenzene or diphenylbutadiene derivatives could be utilized for light induced recording of full color images.[20] Recent studies have shown that inherently photoactive LCs possess several advantages over doped systems.[21,22] Films drawn from inherently photoactive

Chart 1

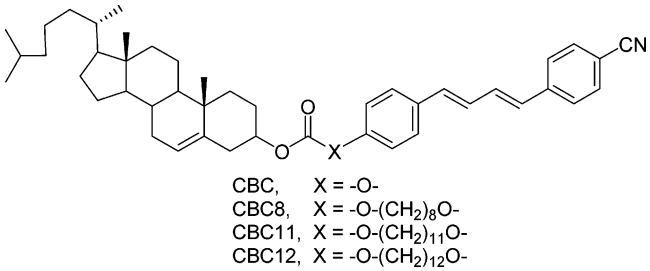

CBC, X = -O-
CBC8, X = -O-$(CH_2)_8$O-
CBC11, X = -O-$(CH_2)_{11}$O-
CBC12, X = -O-$(CH_2)_{12}$O-

LCs essentially consist of pure materials with well-defined molecular weights where the problem of dilution of the photochrome does not exist. This can result in much faster switching times and enhanced stability of the film.[8,22] Our initial effort in the design of inherently photoactive liquid crystals for recording color images met with only a partial success.[23] Although a light induced smectic to N* phase transition was observed in cholesterol−azobenzene linked systems, the rapid thermal cis−trans isomerization of the azobenzene moiety resulted in a loss of the recorded image. Moreover these materials did not form LC stable glasses.

Our continued interest in designing an inherently photoactive glass forming N* LCs leads us to the synthesis of a series of novel asymmetric liquid crystal dimers, consisting of a cholesterol moiety linked to a diphenylbutadiene chromophore (CBCn, Chart 1) via flexible alkyl chains.[24] These liquid crystal dimers possess the combined glass forming properties of the cholesterol moiety and the photochromic and luminescent properties of the butadiene moiety. Photoinduced cis/trans isomerization of the butadiene chromophore in these materials could be utilized to bring about an isothermal phase transition from the smectic to the cholesteric state.[25] By photochemically controlling the cis/trans isomer ratio, the pitch of the cholesteric could be continuously varied making it possible to tune the color of the film over the entire visible region, and the color images thus generated could be stabilized by converting them to N* glasses. These materials were also polymorphic, exhibiting two crystalline forms possessing distinctly different fluorescence properties. The ability to thermally switch these materials from one crystalline form to the other in a reversible manner also makes them useful for recording fluorescent images.

Results and Discussion

Phase Transition Behavior. The mesomorphic properties of the CBC derivatives were investigated by polarized optical microscopy (POM), differential scanning calorimetry (DSC), and small angled X-ray diffraction (XRD). The transition temperatures and corresponding enthalpy values are summarized in Table 1. With the exception of CBC, which decomposed above its isotropization temperature, all the derivatives showed

(9) (a) Moriyama, M.; Mizoshita, N.; Yokota, T.; Kishimoto, K.; Kato, T. *Adv. Mater.* **2003**, *15*, 1335−1338. (b) Gibbons, M.; Shannon, P. J.; Sun, S.-T.; Swetlin, B. J. *Nature* **1991**, *351*, 49. (c) Burnham, K. S.; Schuster, G. B. *J. Am. Chem. Soc.* **1999**, *121*, 10245−10246.
(10) (a) van Delden, R. A.; van Gelder, M. B.; Huck, N. P. M.; Feringa, B. L. *Adv. Funct. Mater.* **2003**, *13*, 319−324. (b) Ikeda, T.; Tsutsumi, O. *Science* **1995**, *268*, 1873−1875.
(11) (a) Tomasulo, M.; Giordani, S.; Raymo, F. M. *Adv. Funct. Mater.* **2005**, *15*, 787−794. (b) Maly, K. E.; Wand, M. D.; Lemieux, R. P. *J. Am. Chem. Soc.* **2002**, *124*, 7898−7899.
(12) (a) Gourevich, I.; Pham, H.; Jonkman, J. E. N.; Kumacheva, E. *Chem. Mater.* **2004**, *16*, 1472−1479. (b) Hikmet, R. A. M.; Kemperman, H. *Nature* **1998**, *392*, 476−479. (c) Kawata, S.; Kawata, Y. *Chem. Rev.* **2000**, *100*, 1777−1788.
(13) (a) Tabe, Y.; Yokoyama, H. *Nat. Mater.* **2003**, *2*, 806−809. (b) Hubert, C.; Rumyantseva, A.; Lerondel, G.; Grand, J.; Kostcheev, S.; Billot, L.; Vial, A.; Bachelot, R.; Royer, P.; Chang, S.-h.; Gray, S. K.; Wiederrecht, G. P.; Schatz, G. C. *Nano Lett.* **2005**, *5*, 615−619. (c) de Jong, J. J. D.; Hania, P. R.; Pugžlys, A.; Lucas, L. N.; de Loos, M.; Kellog, R. M.; Feringa, B. L.; Duppen, K.; van Esch, J. H. *Angew. Chem., Int. Ed.* **2005**, *44*, 2373−2376.
(14) (a) Furumi, S.; Janietz, D.; Kidowaki, M.; Nakagawa, M.; Morino, S.; Stump, J.; Ichimura, K. *Chem. Mater.* **2001**, *13*, 1434−1437. (b) Willets, K. A.; Ostroverkhova, O.; He, M.; Twieg, R. J.; Moerner, W. E. *J. Am. Chem. Soc.* **2003**, *125*, 1174−1175. (c) Kim, J.-M.; Min, S. J.; Lee, S. W.; Bok, J. H.; Kim, J. S. *Chem. Commun.* **2005**, 3427−3429.
(15) Kubo, S.; Gu, Z.-Z.; Takahashi, K.; Fujishima, A.; Segawa, H.; Sato, O. *J. Am. Chem. Soc.* **2004**, *126*, 8314−8319.
(16) (a) Tamaoki, N. *Adv. Mater.* **2001**, *13*, 1135−1147. (b) Yoshioka, T.; Ogata, T.; Nonaka, T.; Moritsugu, M.; Kim, S.-N.; Kurihara, S. *Adv. Mater.* **2005**, *17*, 1226−1229. (c) Hwang, J.; Song, M. H.; Park, B.; Nishimura, S.; Toyooka, T.; Wu, J. W.; Takanishi, Y.; Ishikawa, K.; Takezoe, H. *Nat. Mater.* **2005**, *4*, 383−387.
(17) (a) Imrie, C. T.; Luckurst, G. R. *Handbook of Liquid Crystals*; Demus, D., Goodby, J. W., Gray, G. W., Spiess, H. W., Vill, V., Eds.; Wiley VCH: Weinheim, 1998. (b) Coles, H. J.; Pivnenko, M. N. *Nature* **2005**, *436*, 997−1000. (c) Date, R. W.; Bruce, D. W. *J. Am. Chem. Soc.* **2003**, *125*, 9012−9013. (d) Henderson, P. A.; Imrie, C. T. *Macromolecules* **2005**, *38*, 3307−3311.
(18) (a) Tamaoki, N.; Parfenov, A. V.; Masaki, A.; Matsuda, H. *Adv. Mater.* **1997**, *9*, 1102−1104. (b) Mallia, V. A.; Tamaoki, N. *Chem. Soc. Rev.* **2004**, *33*, 76−84.
(19) (a) Chen, H. P.; Katsis, D.; Mastrangelo, J. C.; Chen, S. H.; Jacobs, S. D.; Hood, P. J. *Adv. Mater.* **2000**, *12*, 1283−1286. (b) Shibaev, P. V.; Madesen, J.; Genack, A. Z. *Chem. Mater.* **2004**, *16*, 1397−1399. (c) Chen, S. H.; Katsis, D.; Schmid, A. W.; Mastrangelo, J. C.; Tsutsui, T.; Blanton, T. N. *Nature* **1999**, *397*, 506−508. (d) Culligan, S. W.; Geng, Y.; Chen, S. H.; Klubek, K.; Vaeth, K. M.; Tang, C. W. *Adv. Mater.* **2003**, *15*, 1176−1180.
(20) (a) Tamaoki, N.; Song, S.; Moriyama, M.; Matsuda, H. *Adv. Mater.* **2000**, *12*, 94−97. (b) Moriyama, M.; Song, S.; Matsuda, H.; Tamaoki, N. *J. Mater. Chem.* **2001**, *11*, 1003−1010. (c) Davis, R.; Mallia, V. A.; Das, S.; Tamaoki, N. *Adv. Funct. Mater.* **2004**, *14*, 743−748.
(21) (a) Yu, Y.; Nakano, M.; Ikeda, T. *Nature* **2003**, *425*, 145. (b) Yagai, S.; Nakajima, T.; Kishikawa, K.; Kohmoto, S.; Karatsu, T.; Kitamura, A. *J. Am. Chem. Soc.* **2005**, *127*, 11134−11139.
(22) (a) Frigoli, M.; Welch, C.; Mehl, G. H. *J. Am. Chem. Soc.* **2004**, *126*, 15382−15383. (b) Tamaoki, N.; Aoki, Y.; Moriyama, M.; Kidowaki, M. *Chem. Mater.* **2003**, *15*, 719−726.
(23) Mallia, V. A.; Tamaoki, N. *Chem. Mater.* **2003**, *15*, 3237−3239.
(24) Supporting Information.
(25) Davis, R.; Mallia, V. A.; Das, S. *Chem. Mater.* **2003**, *15*, 1057−1063.

Table 1. Melting Points, Phase Sequences, Phase Transition Temperatures, and Phase Transition Enthalpy Changes in the Heating and Cooling Cycles of the CBC Derivatives

sample code	heating cycle, °C (ΔH, kJ/mol)	cooling cycle, °C (ΔH, kJ/mol)
CBC	Cr 196.2[a] (21.4) SmA* 239.5[a] (1.9) TGBA* 243.6 N* 264.4[a] dec	
CBC8	Cr_1 99.5[a] (27.2) SmA* 112.8[a] (25.4) Cr_2 131.9[a] (26.2) SmA* 134 TGBA* 138 N* 202.9[a] (3.3) Iso	Iso 193.5[a] (1.1) N* 132 TGBA* 128 SmA* 74.9[a] (24.8) Cr
CBC11	Cr 120.9[a] (36.9) SmA* 145.5[a] (0.03) N* 175.0 (0.13) Iso	Iso162.1[a] (2.1) N* 113.7 (2.1) SmA* 84.9[a] (4.8) Cr
CBC12	$Cr_1$109.4[a] (15.1) SmA* 112.8[a] (19.5) Cr_2 129.5[a] (41.3) N* 188.1[a] (1.8) Iso	Iso 176.6[a] (3.6) N* 108 SmA* 73.9[a] (26.2) Cr

[a] As observed by DSC; Cr, Crystal; SmA*, Chiral smectic A; TGBA*, Twist grain-boundary phase A*; N*, Chiral nematic; and Iso, Isotropic.

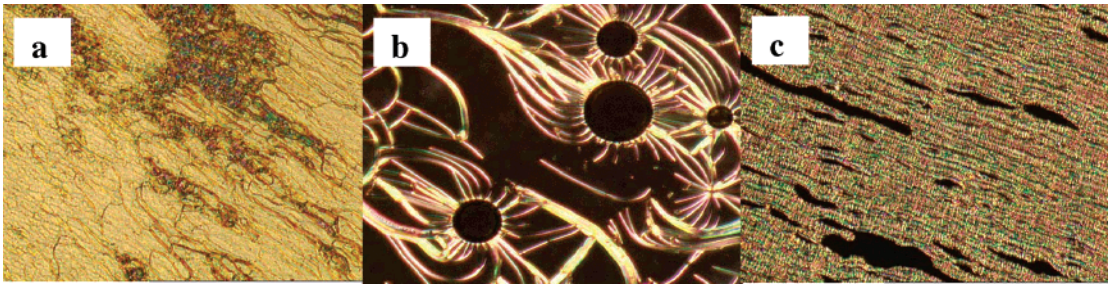

Figure 1. Polarized photomicrographs of CBC8 in (a) N* (152 °C) phase, (b) TGBA* phase (135 °C), and (c) SmA* phase (121 °C).

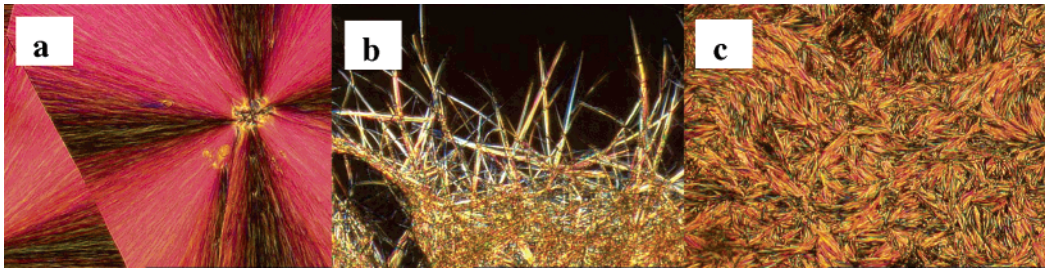

Figure 2. Polarized photomicrographs of CBC8 in (a) crystalline-spherulite (b) growth of crystalline fibers into homeotropic areas, and (c) fiberlike crystal.

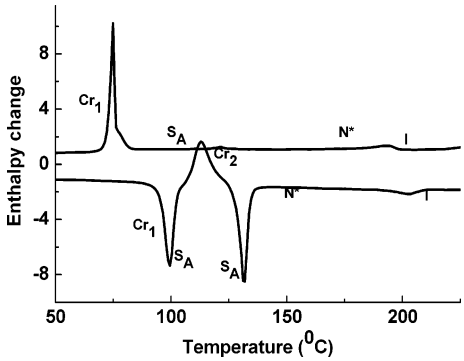

Figure 3. DSC trace of CBC8 in the cooling\heating cycle, rate 5 °C per min.

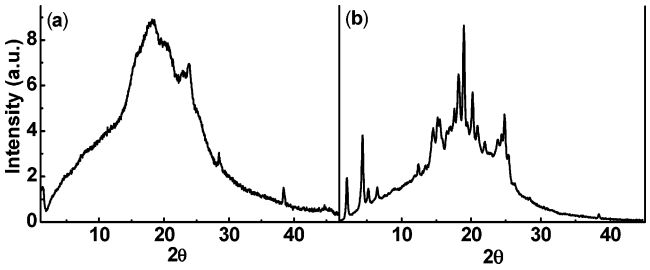

Figure 4. XRD diagram of CBC12 in (a) Cr_1 and (b) Cr_2 phase.

enantiotropic (thermodynamically stable) LC properties exhibiting smectic A* (SmA*)[24] and N* phases. For example, cooling the isotropic liquid of CBC8 resulted in the formation of the N* phase, which could be confirmed by the single color reflecting Grandjean textures, observed using POM (Figure 1a). At 132 °C, a wormlike texture characteristic of the Twist grain-boundary A* (TGBA*) phase was observed (Figure 1b).[26] On further cooling, an SmA* with focal conic patterns with homeotropic domains was observed (Figure 1c). XRD measurements of the SmA* phase show a sharp low angle peak accompanied by a diffuse peak at a wider angle. Interlayer distances (d) calculated from XRD were found to be significantly larger than the calculated dimension of the molecule (L). The d/L values were observed to be ~1.5 indicating an interdigitated layerlike arrangement.[24,27]

An unusual behavior was observed in the phase transition of CBC8 and CBC12 in the heating cycle.[28] On heating a thin film of CBC8, POM studies indicated that the spherulite crystalline texture (Cr_1) observed initially (Figure 2a) melted to form an SmA* phase characterized by its focal conic texture with homeotropic areas.[24] Interestingly, further heating resulted in the unexpected formation of fibrous crystals (Cr_2), which slowly grew into the smectic homeotropic areas (Figure 2b) until complete formation of birefringent fibrous crystals occurred

(26) (a) Goodby, J. W. *J. Mater. Chem.* **1991**, *1*, 307−318. (b) *Textures of Liquid Crystals*; Dierking, I., Ed.; Wiley-VCH: Weinheim, Germany, 2003.

(27) Attard, G. S.; Date, R. W.; Imrie, C. T.; Luckurst, G. R.; Roskilly, S. J.; Seddon, J. M.; Taylor, L. *Liq. Cryst.* **1994**, *16*, 529−581.

(28) Morris, N. L.; Zimmermann, R. G.; Jameson, G. B.; Dalziel, A. W.; Reuss, P. M.; Weiss, R. G. *J. Am. Chem. Soc.* **1988**, *110*, 2177−2185.

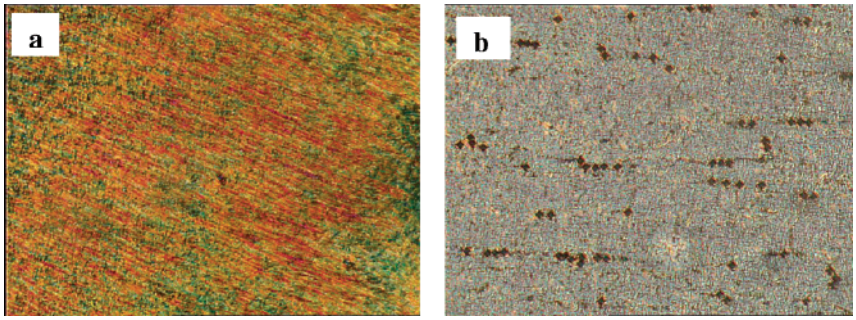

Figure 5. Polarized photomicrographs of CBC12 in (a) N* and (b) SmA* glassy LC state.

(Figure 2c). Samples rigorously purified by HPLC in order to ensure removal of any impurities gave the same results. Similar observations were made in repetitive heating scans.

Subsequent heating of these crystals (Cr_2) resulted in the reappearance of the SmA* phase at 132 °C. The $Cr_1-SmA^*-Cr_2$ transition which was also observed in the heating cycle of CBC12 was reproducible and was observed both for samples crystallized from solvents and for supercooled solids. The transition of the relatively less ordered SmA* phase to highly ordered crystals in the heating cycles of CBC8 and CBC12 was confirmed by DSC, which showed clear endotherms corresponding to the smectic-to-crystal transformations observed by POM (Figure 3).[24] XRD measurements indicated that the interlayer distance (*d*) was the same for the SmA* phases of CBC8 which appear before and after the Cr_2 phase.

An explanation for this unusual behavior can be obtained by studying the XRD patterns of the two crystalline samples. The XRD pattern of Cr_1 was broad, indicative of a glassy nature (Figure 4), suggesting that Cr_1, which is usually obtained by cooling the LC melt, forms a metastable state or "frustrated crystal",[29] where the molecules are not highly ordered. On heating, the sample initially melts to the smectic phase, wherein the molecules have the freedom to move and which on further heating reorient to form highly ordered crystals. The highly crystalline nature of this form is reflected by the sharp peaks observed in its XRD pattern (Figure 4). The two crystalline forms also possessed distinctly different fluorescence properties, and this aspect is discussed later.

Formation of Glassy LCs. The dimesogens CBC8, CBC11, and CBC12 formed stable transparent glassy LCs (Figure 5) when they were suddenly cooled from their LC state to ~0 °C. The glassy LCs obtained by cooling from the LC phases were stable for several months at room temperature. POM studies indicated a glassy LC-to-Cr transition temperature for CBC8, CBC11, and CBC12 at 100 °C, 97 °C, and 105 °C, respectively.

The reflection induced by the helical arrangement in CLCs satisfies the equation $\lambda_{max} = np$, where λ_{max} is the reflection maximum, *p*, the pitch of the helix, and *n*, the refractive index. When $[dp/dt] < 0$, as in the present case, the pitch length decreases with increasing temperature. The reflection band maximum of a CBC12 film shifts from 900 to 560 nm on changing the temperature from 115 °C to 190 °C (Figure 6). Similar effects were observed for the other derivatives. The glassy LCs formed by cooling the cholesteric phase retained the reflection band observed at the temperature from which they were cooled.

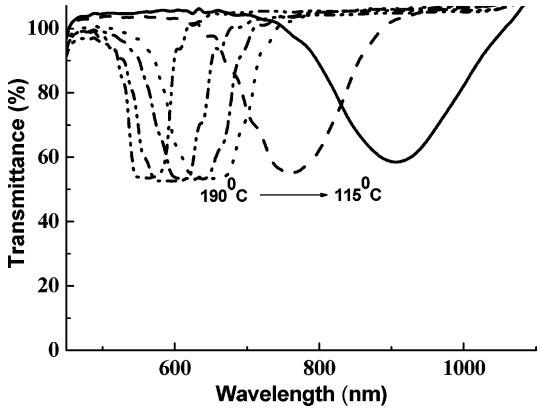

Figure 6. Transmission spectra obtained for a thin-film (10-μm thickness) of CBC12 with decreasing temperature in the cooling cycle.

Photoinduced Isothermal Phase Transitions. Photoisomerization of the diphenyl butadiene chromophore is known to result in the formation of stable cis isomers,[25] and this process could be utilized to bring about light induced isothermal phase transitions in the CBC derivatives. Irradiation with 366 nm light of an SmA* film of CBC12 held at 105 °C resulted in the formation of an N* phase characterized by its Grandjean texture and reflected colors (Figure 7b), while prolonged irradiation lead to isotropization.

The pitch of the N* formed on photoirradiation was observed to decrease with an increase in the time or intensity of irradiation (Figure 8), making it possible to tune the color of the film over the entire visible range. Using this procedure, color images could be recorded in the cholesteric films and the images thus formed could be stabilized by rapidly quenching the temperature of the irradiated film to ~0 °C.

Photoisomerization of the all trans isomer of donor/acceptor (D/A) substituted alkoxy diphenyl butadienes has been earlier reported to result in the formation of thermally stable EZ and ZE (cis isomers), which were separated by HPLC and characterized.[25] Similarly analysis of the irradiated samples of the mesogenic dimers used in the present study also indicated the formation of the EZ and ZE isomers (Figure 9). By analogy with earlier studies the first peak in the HPLC trace may be attributed to the formation of the EZ isomer and the second peak to that of the ZE isomer.

The total amount of the cis isomers formed on photoirradiation of CBC12 in its liquid crystalline phases at various irradiation times was determined by HPLC in order to understand its effect on the phase transition characteristics. Thin

(29) (a) Jung, H.-T.; Hudson, S. D.; Lenz, R. W. *Macromolecules* **1998**, *31*, 637−643. (b) Ye, C.; Xu, G.; Yu, Z.-Q.; Lam, J. W. Y.; Jang, J. H.; Peng, H.-L.; Tu, Y.-F.; Liu, Z.-F.; Jeong, K.-U.; Cheng, S. Z. D.; Chen, E.-Q.; Tang, B. Z. *J. Am. Chem. Soc.* **2005**, *127*, 7668−7669.

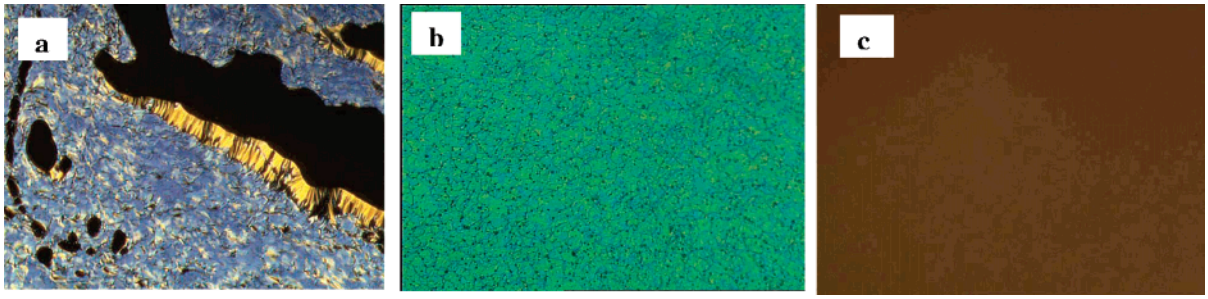

Figure 7. Polarized photomicrographs of CBC12 at 105 °C (a) before irradiation (SmA*), (b) after irradiation for 15 s (N*), and (c) after irradiation for 9 min (isotropic phase) with 366 nm light.

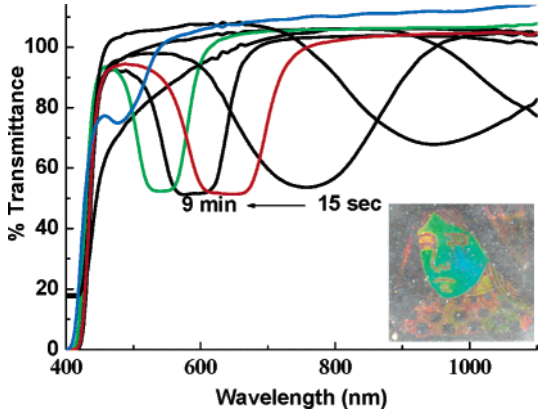

Figure 8. Changes in reflection band of the cholesteric phase of CBC12 developed on photoirradiation of its smectic film held at 105 °C. Inset shows an image stored in a cholesteric glass, obtained by energy modulated irradiation of a smectic film at 105 °C followed by temperature quenching to ~0 °C .

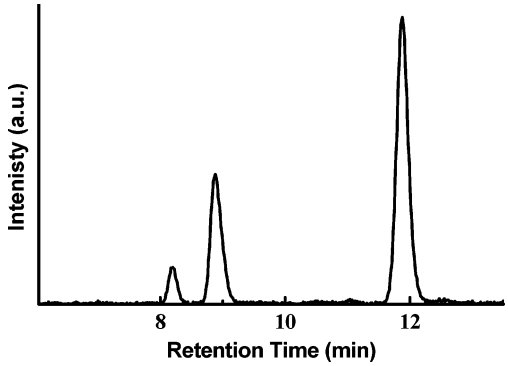

Figure 9. HPLC trace of CBC12 in isotropic state formed from smectic state by photoirradiation with 366 nm light.

smectic films of CBC12 held at 105 °C between two cover slips separated by a 10 μm spacer were irradiated using 366 nm light for different intervals of time. Figure 10 shows the dependence of the phase transition of CBC12 on the amount of cis isomers formed as a result of irradiation for different periods of time. At 105 °C it was observed that 1% conversion to the cis isomers was sufficient to bring about an SmA* to N* transition, whereas 21% conversion to cis isomers was required to induce isotropization. The SmA* phase was not observed in samples containing more than 5% of the cis isomers.

A schematic representation of the photoinduced effect is shown in Figure 11. On photoirradiation, formation of the cis isomers initially destabilizes the SmA* phase, bringing about a reduction in the SmA*-to-N* phase transition temperature. With increasing concentration of the cis isomers, the pitch of the

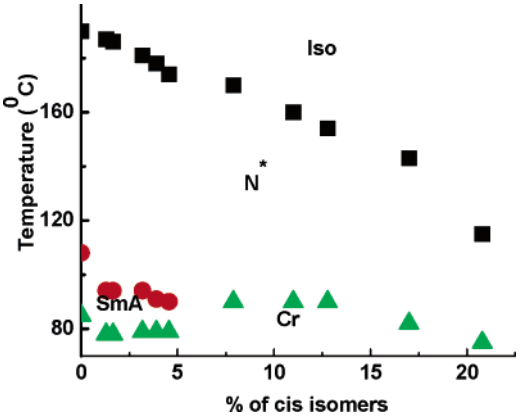

Figure 10. Binary phase diagram obtained by the photogeneration of cis isomers of CBC12 in the cooling cycle

cholesteric phase decreases resulting in a blue shift in its reflection band. At high cis concentrations, an isothermal phase transition to the isotropic phase occurs. The isotropization temperature was lowered by ~90 °C, which is substantially larger than any of the previous reports on photoresponsive LCs.[23,30]

Although the photogenerated cis isomers were thermally stable, they could be reverted back to the all trans form by irradiating with 266 nm light. It is well-known that in polyenes and related systems trans−cis photoisomerization is prevented in a rigid media, whereas cis−trans photoisomerization remains feasible, resulting in stereospecific isomerization.[31] Thus 266 nm photoirradiation of film containing a mixture of the cis and trans isomers in the solid state results in near complete recovery of the all trans isomer (Figure 12). Using this procedure the images recorded using 366 nm light could be erased by irradiating them with 266 nm laser light.

Solid State Fluorescence and Thermal Imaging. There is a growing interest in the development of materials whose solid state luminescent properties can be reversibly controlled using external stimuli.[10,32] The two polymorphic crystalline forms of CBC8 and CBC12 possess significantly different fluorescence properties, which could be attributed to differences in the molecular packing of the two forms. The effect of temperature on the solid-state optical properties was investigated in order to gain an insight into the nature of these differences. The absorption spectra of a film of CBC12 cast on quartz plates

(30) Kumaresan, S.; Mallia, V. A.; Kida, Y.; Tamaoki, N. *J. Mater. Res.* **2005**, *20*, 3431−3438.
(31) (a) Liu, R. S. H. *Acc. Chem. Res.* **2001**, *34*, 555−562. (b) Sun, Y.-P.; Saltiel, J.; Hoburg, E. A.; Waldeck, D. H. *J. Phys. Chem.* **1991**, *95*, 10336−10344. (c) Liu, R. S. H.; Asato, A. E.; Denny, M. *J. Am. Chem. Soc.* **1983**, *105*, 4829−4830.

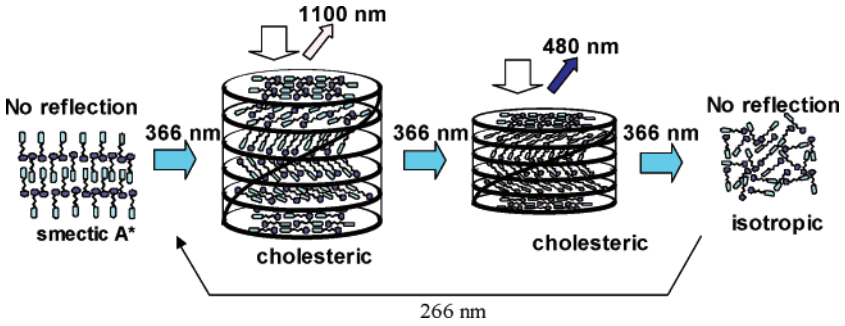

Figure 11. Schematic representation of photoinduced isothermal phase transition from SmA* to isotropic phase via the N* phase

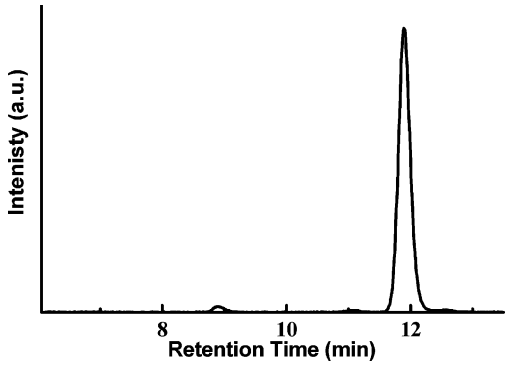

Figure 12. HPLC trace of CBC12 in recovered all trans state obtained by reverse isomerization in solid state using 266 nm laser.

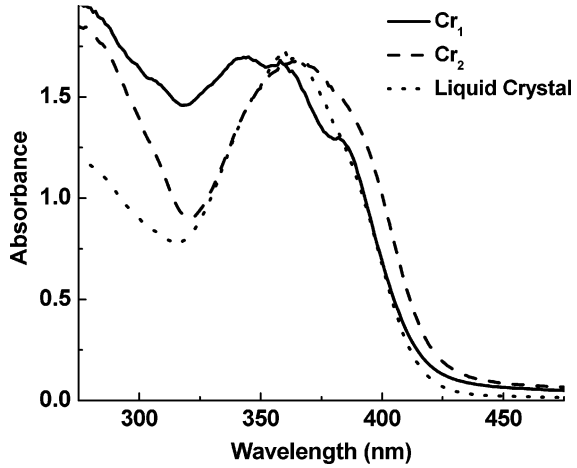

Figure 13. Normalized absorption spectra of CBC12 in (a) Cr_1, (b) Cr_2, and (c) liquid crystalline states.

were recorded between 100 and 120 °C, where the compound exists in its Cr_2 form. The spectrum indicates a peak at 360 nm, similar to that observed in the LC phase (Figure 13). The absorption spectrum is also very similar to that observed in toluene solutions,[24] indicating that the main absorbing species in the crystal and in the LC phase is the monomer. In contrast, at lower temperatures where CBC12 exists in its Cr_1 form, the absorption spectra of the film exhibited a broad band with

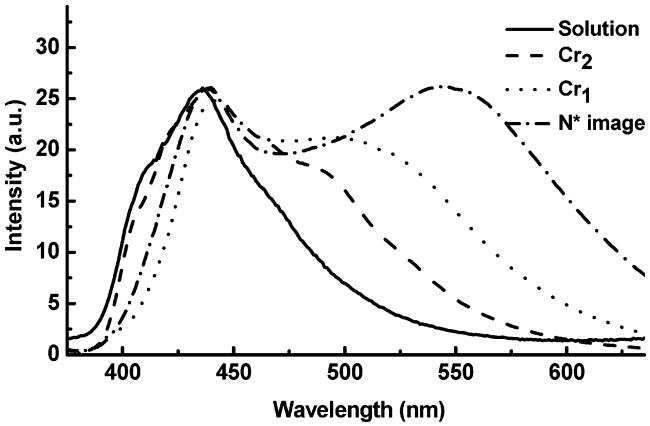

Figure 14. Fluorescence spectra of CBC12 in (a) solution state, (b) Cr_1, (c) Cr_2, and (d) cholesteric image.

maxima at 342 and 359 nm and a shoulder at 383 nm. These results point to the existence of spectroscopically different states. In bulk materials, the tendency to form aggregates is very high. Interaction between chromophores in their ground state on aggregation has been fairly well explained by McRae and Kasha in terms of exciton coupling theory.[33] The excited state of aggregates is split into two energy levels (Davydov splitting). The transition to the upper state is allowed in the case of H-aggregates and is characterized by a hypsochromically shifted absorption band, while the transition to the lower state is allowed for J-aggregates and is marked by a bathochromically shifted absorption band compared with the isolated monomer. The multiple absorption peaks observed for Cr_1 indicates formation of both H- and J-type aggregates. The glassy nature of Cr_1 indicated by its X-ray diffraction pattern could therefore be attributed to the existence of such different types of interchromophore arrangements.[34]

Evidence for differences in the molecular packing in Cr_1 and Cr_2 was also obtained from their fluorescence spectra. Figure 14 shows the normalized solid-state emission spectra of CBC12 in its Cr_1, Cr_2, and glassy cholesteric forms. The emission spectrum of CBC12 in toluene solution is also shown for comparison. The short wavelength band with its maximum centered on 438 nm can be attributed to emission of the monomer, while the long wavelength band observed in the 475

(32) (a) Deans, R.; Kim, J.; Machacek, M. R.; Swager, T. M. *J. Am. Chem. Soc.* **2000**, *122*, 8565−8566. (b) Precup-Blaga, F. S.; Garcia-Martinez, J. C.; Schenning, A. P. H. J.; Meijer, E. W. *J. Am. Chem. Soc.* **2003**, *125*, 12953−12960. (c) Mutai, T.; Satou, H.; Araki, K. *Nat. Mater.* **2005**, *4*, 685−687. (d) Kishimura, A.; Yamashita, T.; Yamaguchi, K.; Aida, T. *Nat. Mater.* **2005**, *4*, 546−549. (e) Hulvat, J. F.; Sofos, M.; Tajima, K.; Stupp, S. I. *J. Am. Chem. Soc.* **2005**, *127*, 366−372. (f) Lim, S.-J.; An, B.-K.; Jung, S. D.; Chung, M.-A.; Park, S. Y. *Angew. Chem., Int. Ed.* **2004**, *43*, 6346−6350. (g) Sheikh-Ali, B. M.; Weiss, R. G. *J. Am. Chem. Soc.* **1994**, *116*, 6111−6120.

(33) (a) Dellinger, B.; Kasha, M. *Chem. Phys. Lett.* **1976**, *38*, 9−14. (b) McRae, E. G.; Kasha, M. *Physical Processes in Radiation Biology*; Augenstein, L., Mason, R., Rosenberg, B., Eds.; Academic Press: New York, 1964; p 23.

(34) (a) Robinson, M. R.; Wang, S.; Heeger, A. J.; Bazan, G. C. *Adv. Funct. Mater.* **2001**, *11*, 413−419. (b) Fu, H.; Loo, B. H.; Xiao, D.; Xie, R.; Ji, X.; Yao, J.; Zhang, B.; Zhang, L. *Angew. Chem., Int. Ed.* **2002**, *41*, 962−965.

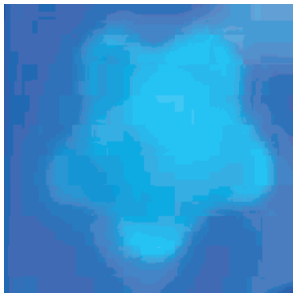

Figure 15. Fluorescent image of CBC12 obtained by placing a hot object, which was then removed, on the blue fluorescent crystalline material (under 365 nm illumination).

to 650 nm region can be attributed to emission of the aggregate.[35] From the figure it is clear that the contribution of emission from the aggregate is significantly less for Cr_2, whereas for Cr_1 and the glassy cholesteric film the aggregate emission is substantial.

The differences in the fluorescence of Cr_1 with that of Cr_2 and the glassy cholesteric film was visually perceivable making it possible to record fluorescent images on these materials. Figure 15 shows the fluorescent image recorded on a thin film of Cr_2 of CBC12, by momentarily placing a hot object on the film. The object was placed for a sufficient time to allow transformation of the Cr_2 to the N* phase in the heated regions. Removal of the object leads to rapid cooling, resulting in the formation of a glassy N*. The fluorescence spectrum of the heated region was similar to that shown in Figure 14, curve d. Using this procedure a variety of images could be recorded on the films. Erasure of the image could be achieved by following a heating−cooling cycle, which allowed regeneration of the Cr_2 form.

(35) (a) Davis, R.; Rath, N. P.; Das, S. *Chem. Commun.* **2004**, 74−75. (b) Davis, R.; Abraham, S.; Rath, N. P.; Das, S. *New J. Chem.* **2004**, *28*, 1368−1372.

Conclusion

The mesogenic dimers described here form a versatile class of materials with multifunctional properties. These inherently photoresponsive liquid crystals form stable, clear N* glasses and also possess polymorphic crystalline forms with visually distinguishable fluorescence. These properties make them useful for photochemical and thermal recording of full color and fluorescent images in a reversible manner. The photoinduced drop in the N*−I transition of 90 °C is the highest reported for photoresponsive liquid crystals.

Acknowledgment. The research fellowship from the Japanese Society for Promotion of Science (JSPS) and the travel support from the Department of Science and Technology (DST), India under an Indo-Japanese Scientific Collaborative Project (IJSCP) program are gratefully acknowledged. This is Contribution No. 217 from RRLT-PPD.

Supporting Information Available: Details of synthesis, analytical, and spectral characterization data of compounds, *d* spacing from X-ray measurements, and DSC thermogram of CBC11. This material is available free of charge via the Internet at http://pubs.acs.org.

JA061575K